Supporting Information

Solution-processable robust, recyclable and sustainable cellulose conductor for photoelectric devices via starch-gluing-Ag nanowires strategy

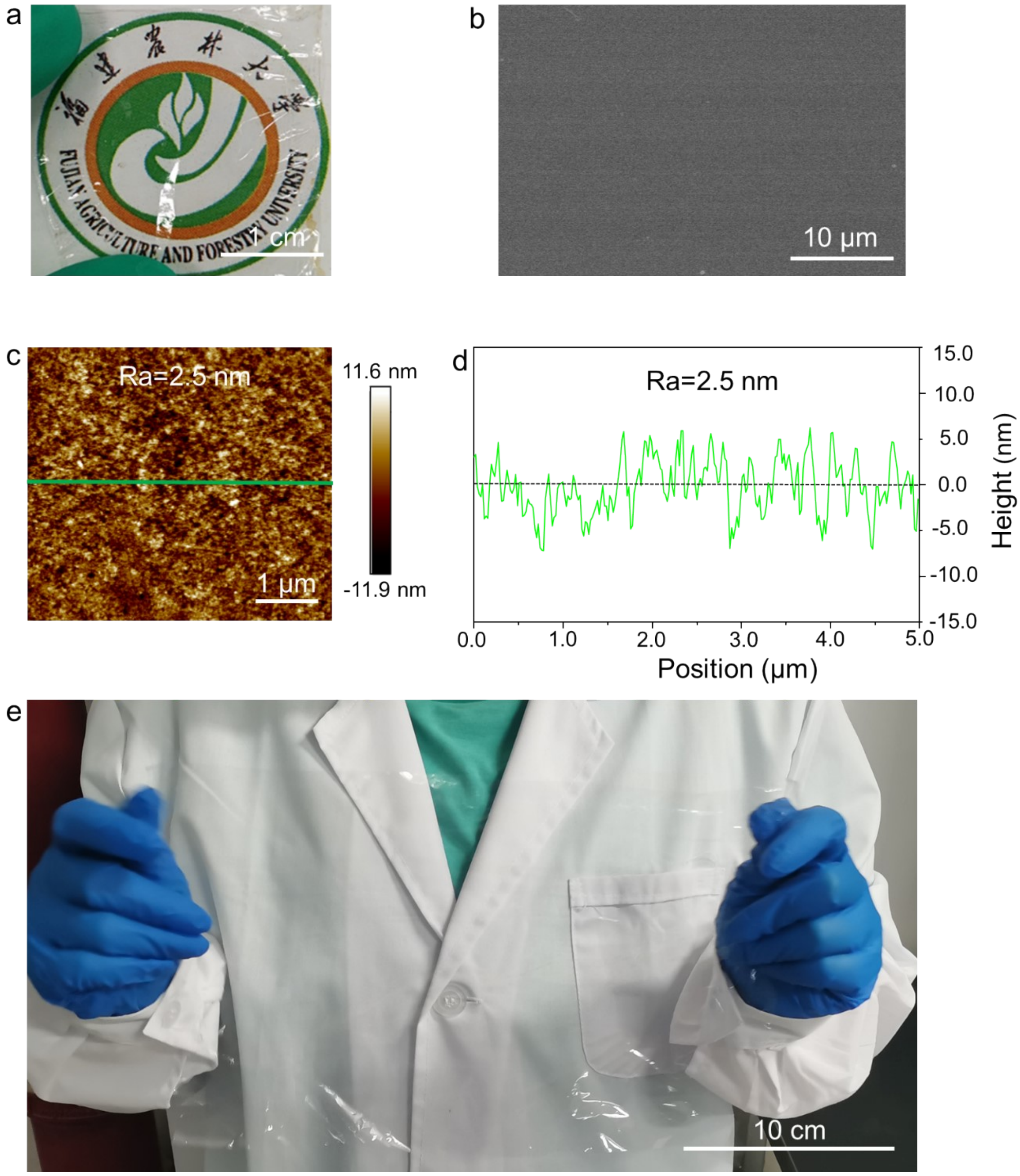

Figure S1. The surface morphologies of pristine cellulose film. (a) Photograph of the pristine cellulose film with a smooth, flat surface. (b) Surface observation of the pristine cellulose film. (c) AFM observation and (d) Height data of the pristine cellulose film. (e) Photograph of the pristine cellulose film.

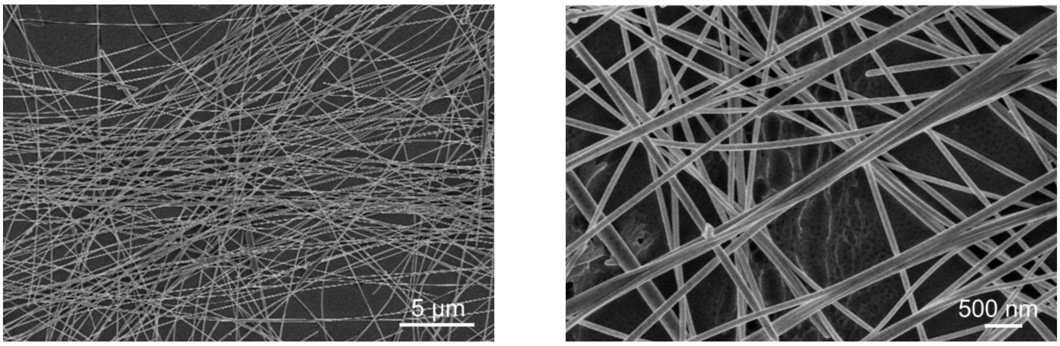

Figure S2. Observation of the surface of CA film.

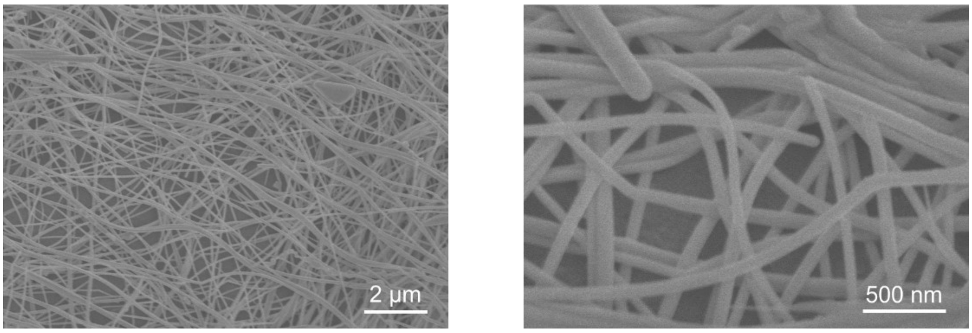

Figure S3. Observation of the surface of CSA film.

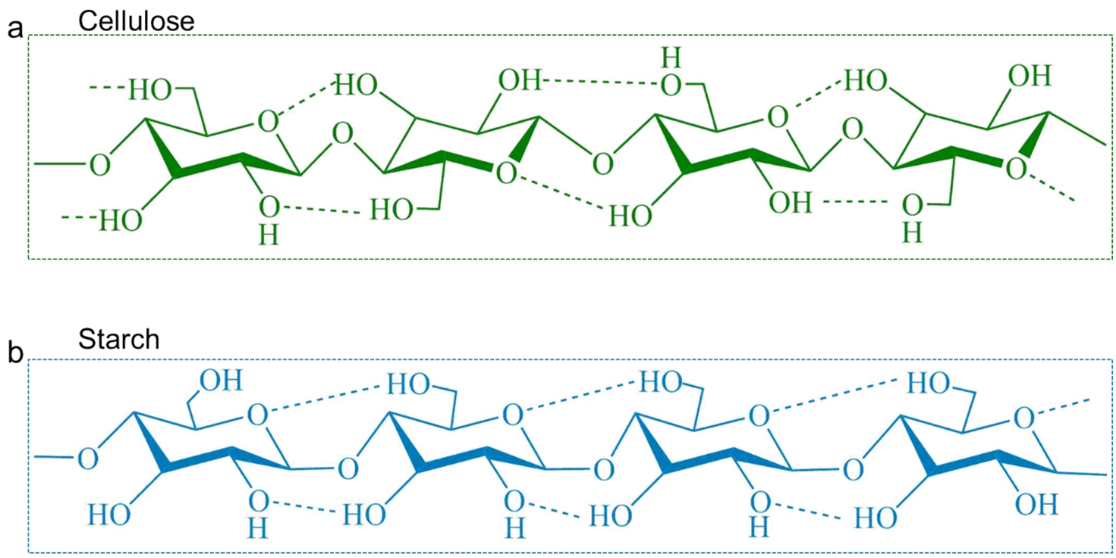

Figure S4. The molecular structure of cellulose (a) and starch (b).

Table S1. The EDS analysis of the CSA film

Sample/element (wt%)	CSA film
C	32.21
O	25.63
Ag	42.14
Total	100.00

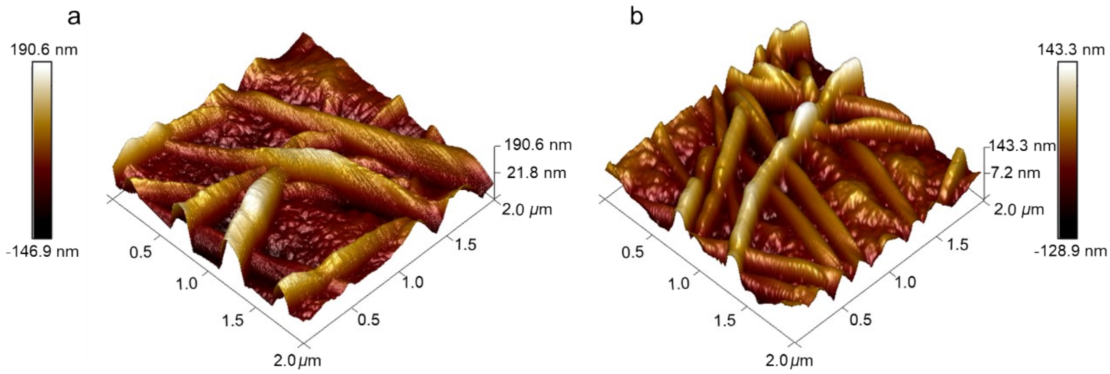

Figure S5. Three-dimensional topographical images of the CA (a) and CSA films (b).

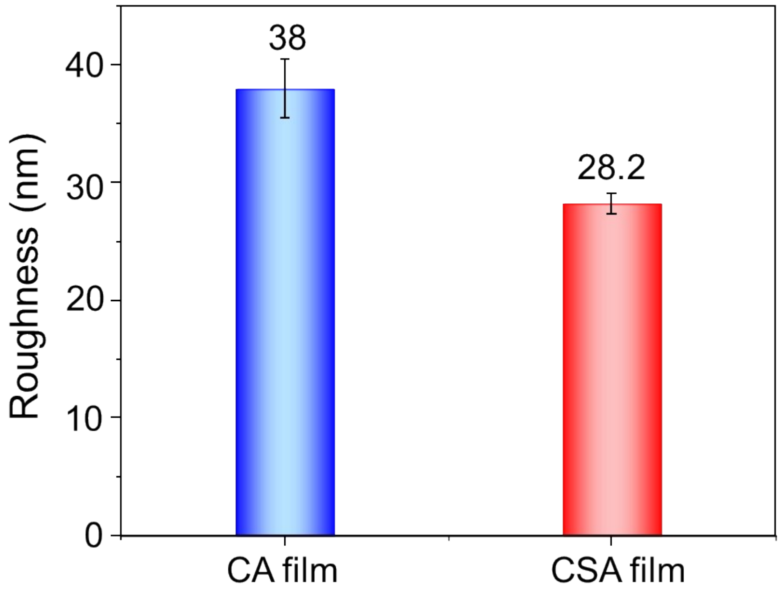

Figure S6. Surface roughness of the CA and CSA films.

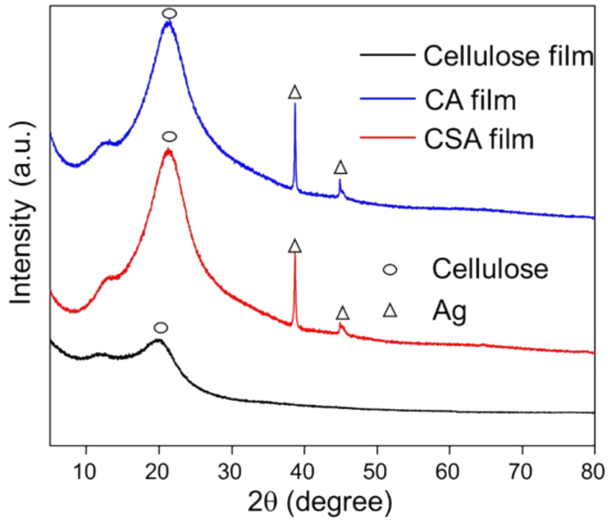

Figure S7. XRD results of the Cellulose, CA and CSA films.

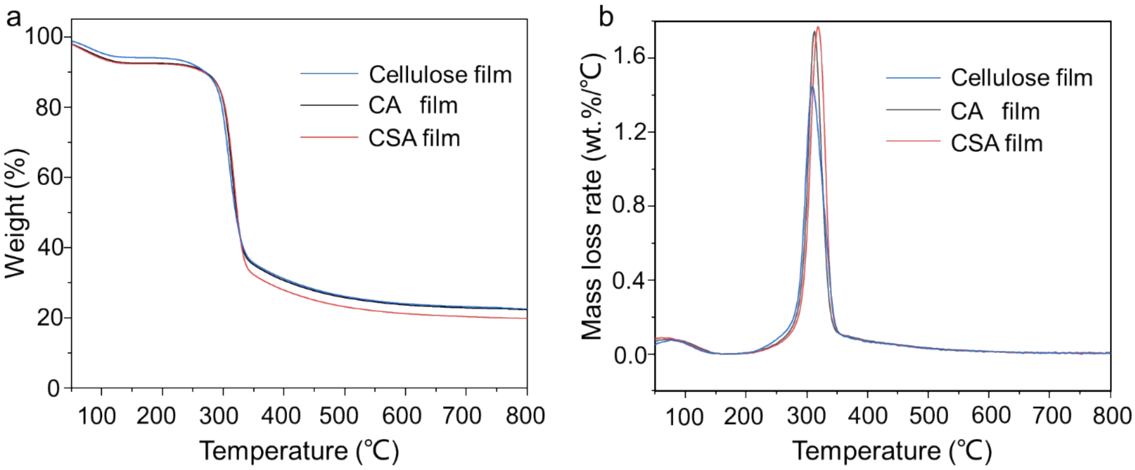

Figure S8. The thermogravimetric analysis of the sample, including weight change (a) and mass loss rate (b).

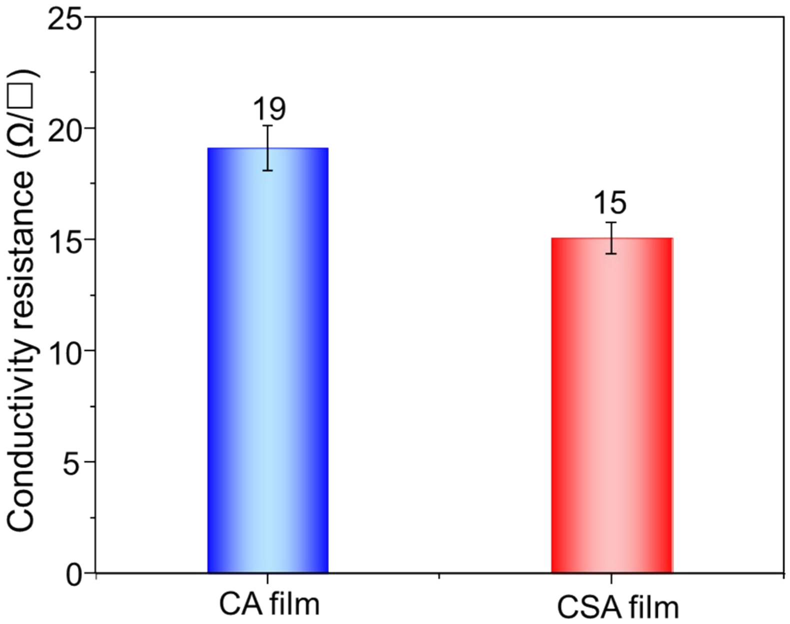

Figure S9. The original conductivity resistance of the CA and CSA films.

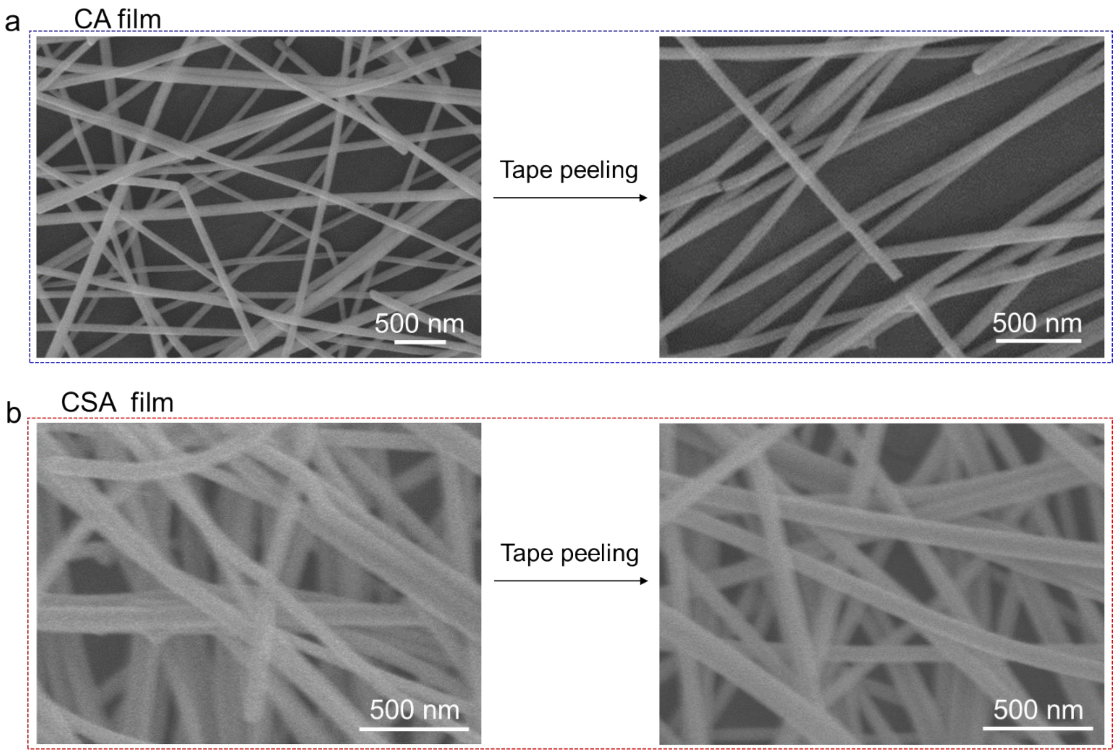

Figure S10. Surface morphology observation of cellulose conductive films after tape peeling treatment, including CA film (a) CSA film (b).

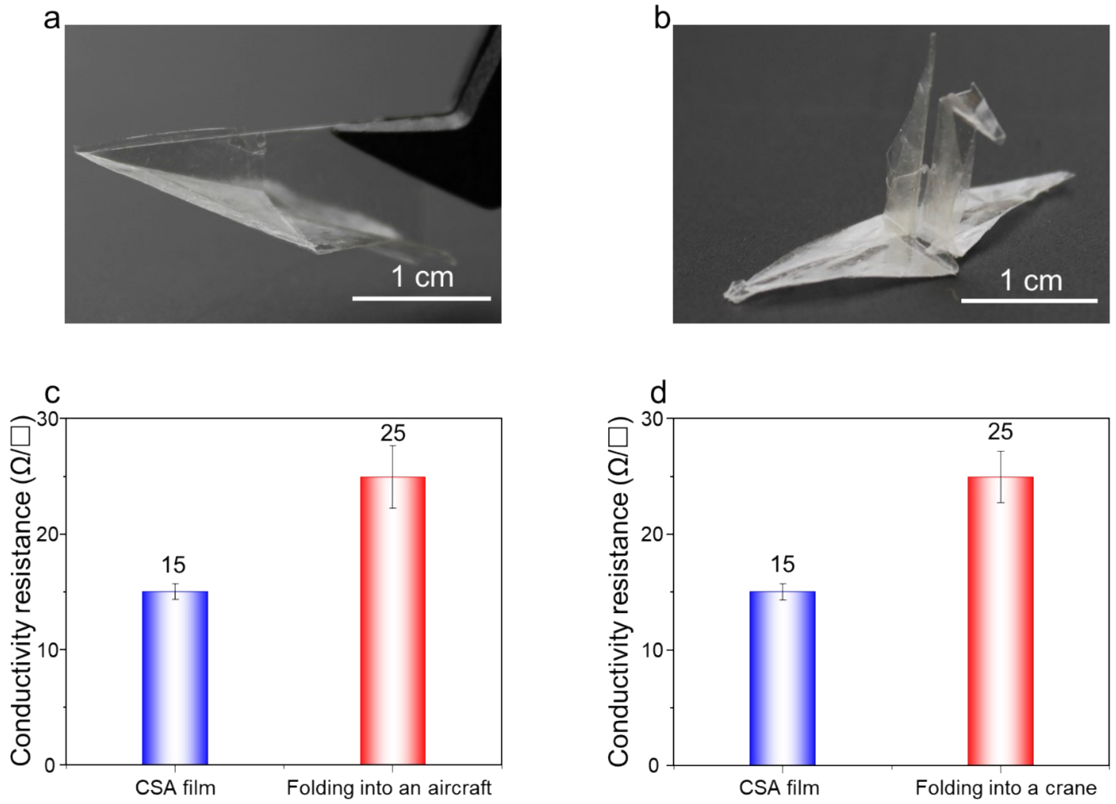

Figure S11. The foldability of the CSA film. (a, b) we can fold the CSA film into various shapes, including aircraft shape (a) and crane shape (b). (c, d) The conductive resistance of CSA film with various shapes, including aircraft shape (c) and crane shape (d).

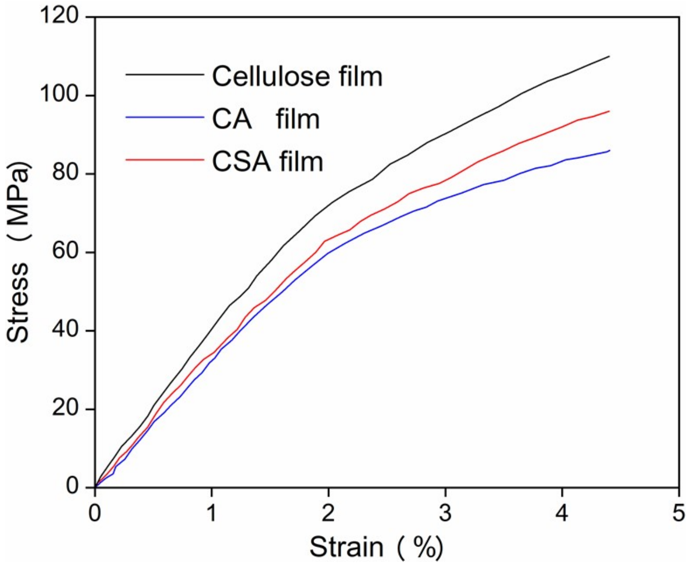

Figure S12. The mechanical strength of cellulose film and cellulose conductive films.

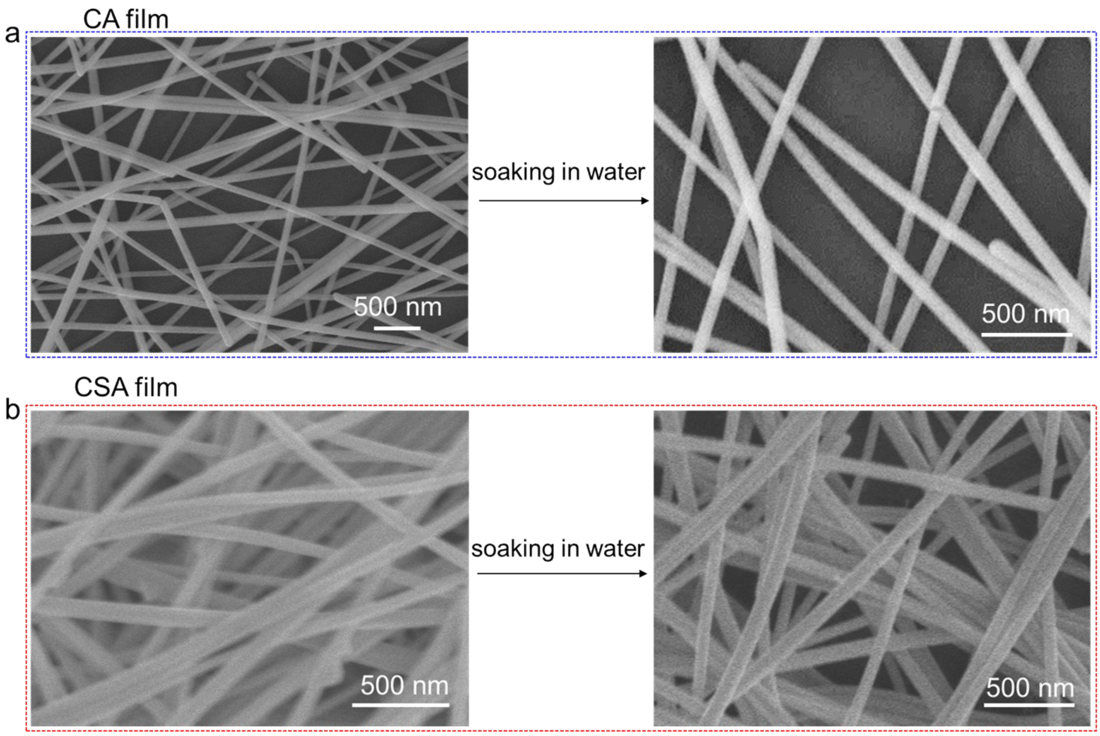

Figure S13. Surface morphology observation of cellulose conductive films after water soaking treatment, including CA film (a) CSA film (b).

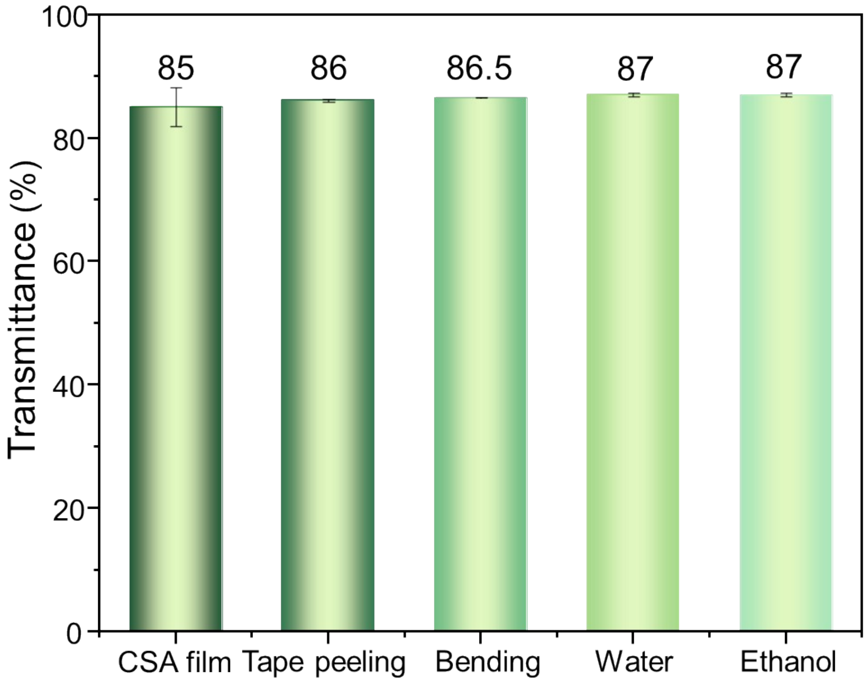

Figure S14. The transmittance of the CSA film after the dramatic treatments.

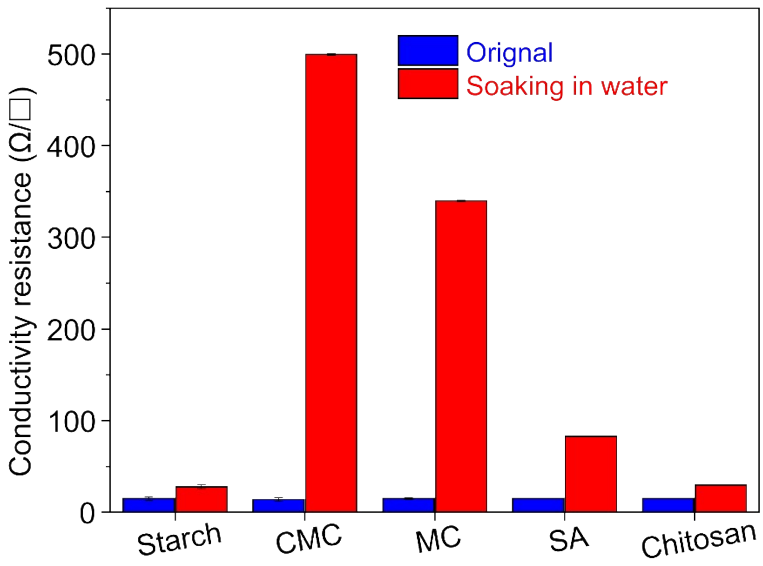

Figure S15. The conductive performance of CSA film with different natural polymers. (CMC: sodium carboxymethyl cellulose, HC: hydroxyethyl cellulose, SA: sodium alginate)

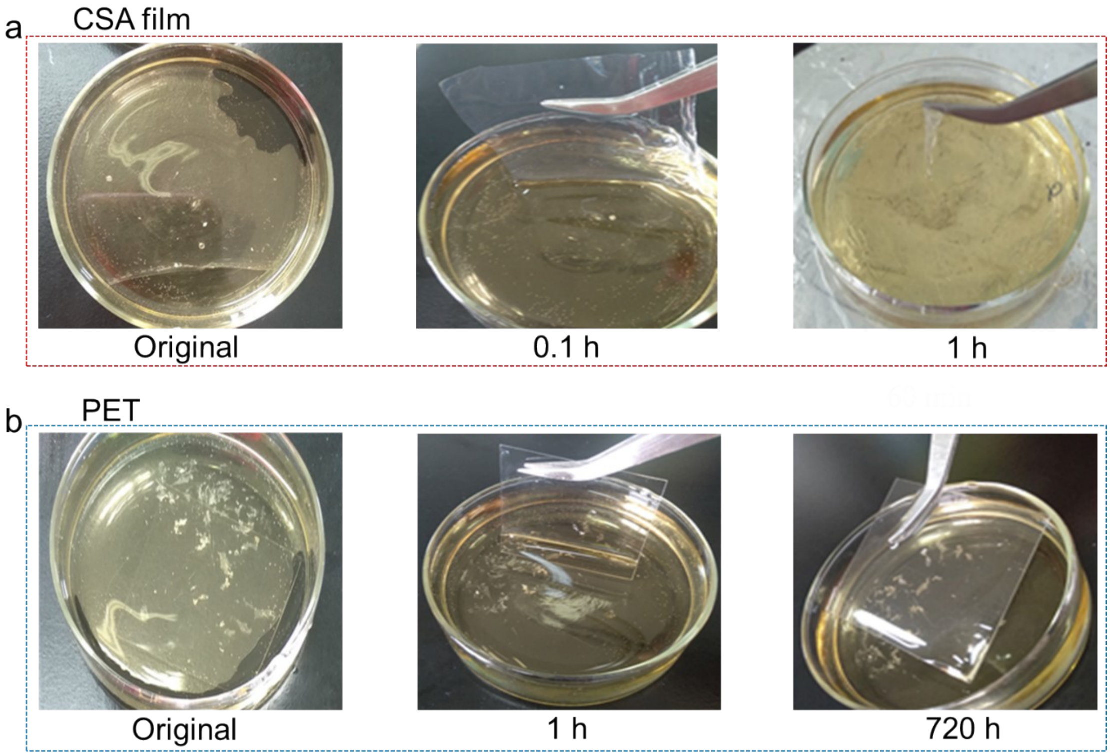

Figure S16. The biodegradability of CSA film (a) and PET (b) in the cellulase solution.

Figure S17. The degradability tests of the cellulose film on grass. Direct outdoor exposure was carried out to evaluate the degradability of the cellulose film, which was placed on grass and exposed to the sun, wind, and rain (Fujian Agriculture and Forestry University, from May 20, 2021, to June 20, 2021). After one day, the dimensions of the cellulose film increased as it became more swollen. After ten days, the cellulose film became cracked and fragmented and its original structure completely degraded after thirty days.

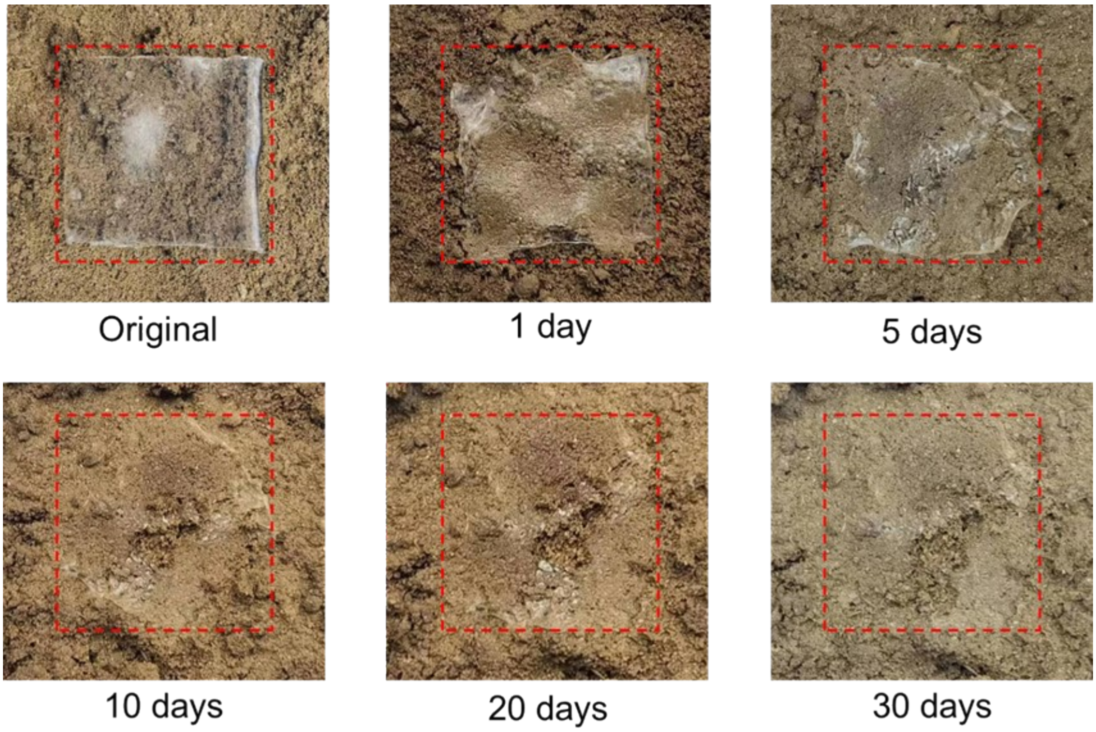

Figure S18. The degradability tests of the cellulose film in the soil at a depth of 5 cm. The robust and stable cellulose film shows good biodegradability in the soil (Fujian Agriculture and Forestry University, from May 20, 2021, to June 20, 2021). After one day, the dimensions of the cellulose film increased as it became more swollen. After five days, the cellulose film became curled and distorted. After ten days, the cellulose film became cracked and fragmented and its original structure completely degraded after thirty days.

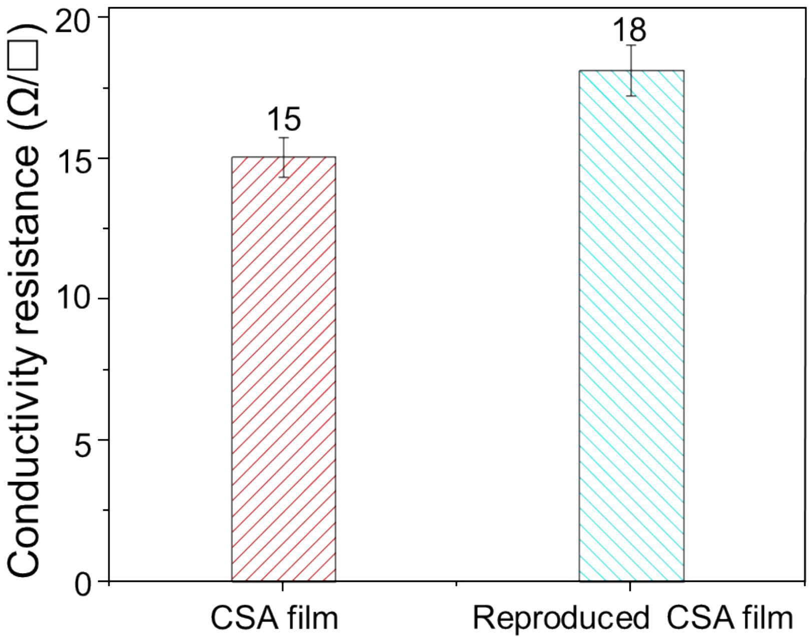

Figure S19. The conductive resistance of the original CSA film and reproduced CSA film with recycled cellulose film and AgNWs.

Figure S20. The organic light-emitting diode is prepared based on the CSA film.